Mem. S.A.It. Suppl. Vol. 15, 166

Memorie della
Supplementi

The geometry of the broad line region: an inflow and accelerating outflow

D. Ilić[1], L.Č. Popović[2], A.I. Shapovalova[3], A. Kovačević[1], J. León-Tavares[4], and V.H. Chavushyan[5]

[1] Department of Astronomy, Faculty of Mathematics, University of Belgrade, Studentski trg 16, 11000 Belgrade, Serbia; e-mail: dilic@matf.bg.ac.rs
[2] Astronomical Observatory Belgrade, Volgina 7, 11060 Belgrade, Serbia
[3] Special Astrophysical Observatory of the Russian Academy of Science, Nizhnij Arkhyz, Karachaevo-Cherkesia 369167, Russia
[4] Metsähovi Radio Observatory, Helsinki University of Technology TKK, Metsähovintie 114, FIN-02540 Kylmälä, Finland
[5] Instituto Nacional de Astrofísica, Óptica y Electrónica, Apartado Postal 51, CP 72000, Puebla, Pue. México

Abstract. The geometry and kinematics of the broad line region (BLR) of active galactic nuclei (AGN) is believed to be very complex and that many different motions are present, which can be seen from the complex profiles of the broad emission lines that are present in the AGN spectra. We will discuss here the problems of the geometry of the BLR and give one possible scenario, such as the possibility that in the BLR there is a dominating accelerating outflow together with an inflow of matter. We apply the model to the real case of the variable AGN NGC 4151, where this model can describe the line profiles in different epochs.

Key words. galaxies: active – (galaxies:) quasars: emission lines

1. Introduction

The broad line region (BLR) is located in the inner regions of active galactic nuclei (AGN), very close to the influence of the supermassive black hole, that is believed to be in the center of AGN. The broad emission lines (BELs), that are produced in the BLR, have profiles that are usually very complex, showing a non-Gaussian shape with some characteristic features (e.g. asymmetries or bumps). Moreover, the BELs are usually variable over long time scales both in flux and profile (see e.g. Shapovalova et al. 2008, 2009a,b). Thus, the BLR is most likely a complex region of which the geometry may vary. Many different models have been proposed to explain the kinematics and geometry of the BLR (e.g. biconical ejection, disk wind, combination of the disk-like and spherical component etc.), and we still have no self-consistent model that would explain the kinematics of the BLR (Peterson 2006). Since there are indications that some of the BLR properties may be related to outflows and jets originated from a close vicinity of the black

Send offprint requests to: D. Ilić

hole and accretion disk (e.g. Arshakian et al. 2009), we study here the possibility of an acceleration outflow having a major influence to the velocity field of the BLR. First ideas of this model appeared in Ilić et al. (2008), and here we proceed with the further development of the model of the BLR geometry.

One of the most famous and best studied Seyfert galaxies is NGC 4151 (see e.g. Ulrich 2000; Sergeev et al. 2001; Shapovalova et al. 2008, and reference therein). This galaxy, and its nucleus, has been studied extensively at all wavelengths. Its interesting features are highly variable BEL profiles (Shapovalova et al. 2008, 2009a,b). Although the AGN of NGC 4151 has been much observed and discussed, there are still several questions concerning the BLR kinematics, dimensions, and physics of the innermost region. For that reason, we apply here the BLR geometry model to the observed Hα line of NGC 4151, and discuss the results.

2. An outflow model in the BLR

In some cases, the broad lines may be formed in the following scenario (see also Fig. 1): there is an outflow in the BLR, the material starts to accelerate close to the black hole, but at the beginning the outflow velocities are small ($V_r \approx 0$), then the emission is affected by a strong gravitational field (i.e. strongly redshifted) so we have the inflow of matter, and the main heating mechanism could be photoionization. Consequently this part contributes to the red wing.

As the acceleration increases, the contribution of the emission shifts to the blue part (conversion of the kinetic energy into thermal one becomes more effective, then excitation is partly produced by internal shock mechanism and partly by photoionization).

At the end, when the velocity of the outflow reaches its maximum, this emission contributes to the far blue wing (and probably excitation is due to the internal shocks). In this part the contribution of photoionization may be negligible (such a situation is observed in NGC 4151, see Shapovalova et al. 2009b), explaining that the

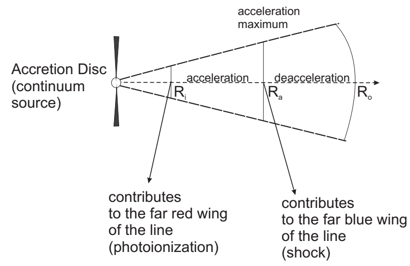

Fig. 1. The scheme representing the outflow in the BLR.

flux of the far blue wing does not respond to the continuum flux variation.

2.1. The model

To apply this scenario to the line profiles, we developed a model which takes into account different velocities, both due to an acceleration outflow and gravitational inflow. This model is the further development of the outflow model presented in Ilić et al. (2008).

In this part we give a simple model taking into account only kinematics projected on the line-of-sight to the observer. The reference frame is defined in such a way that the outflow velocities are approaching velocities, thus negative, while the velocity due to the strong gravitational field is positive. The aim of the fitting is, in the first order, to qualitatively explain different line shapes, and also to get some kinematical parameters.

The accelerating outflow is extending from an inner radius R_i to an outer radius R_o (Fig. 1). We assume that the outflow starts within a few tens of the gravitational radii, R_g, from the central black hole and that its velocity $V(r)$ can be described as a function of the distance, r, from the black hole

$$V(r) = -V_0 \left(\frac{R_i}{r}\right)^{p_1} \quad (1)$$

where V_0 is the initial velocity at R_i and p_1 is a power-law index which is negative in the case of the accelerating outflow. Assuming that the acceleration stops at a radius R_a from the black

Table 1. Model fitting results for the averaged Hα profiles of NFC 4151 for different three periods: I, II and III (see Shapovalova et al. 2008, 2009a,b). R_i is the inner radius of the emitting region, R_o is the outer radius, R_a is the radius where acceleration stops, R_e is the radius after which emission is decreasing, $V_\mathrm{ran}^\mathrm{max}$ is the starting random velocity, $V(R_\mathrm{a})$ is the velocity at the maximum of the accelerating outflow, p_1, p_2, p_3 are the power law indexes of the velocity distributions of accelerating outflow, de-accelerating outflow and emissivity distribution, respectively, and ε_0 is the emissivity constant.

Period	R_i [R_g]	R_o [R_g]	R_a [R_g]	R_e [R_g]	$V_\mathrm{ran}^\mathrm{max}$/c	$V(R_\mathrm{a})$ [km s^{-1}]	p_1	p_2	p_3	ε_0
I	55	1050	322	290	.0044	4250	-4.5	3.6	2.85	.0007
II	40	1600	236	250	.0048	4400	-4.5	4.2	2.90	.0010
III	50	810	270	162	.0053	4900	-4.8	2.5	1.56	.0007

hole (Fig. 1), we can expect that for $r > R_\mathrm{a}$ the velocity of the outflow is decreasing, with a different power-law index p_2, this time positive, as

$$V(r) = -V(R_\mathrm{a})\left(\frac{R_\mathrm{a}}{r}\right)^{p_2} \tag{2}$$

where $V(R_\mathrm{a})$ is the radial velocity at R_a, which can be calculated from

$$V(R_\mathrm{a}) = V_0\left(\frac{R_\mathrm{i}}{R_\mathrm{a}}\right)^{p_1} \tag{3}$$

As we have some distribution of emitters across the outflow, we assume that the brightness of the outflowing material is strong and flattens up to a radius R_e, i.e. $\varepsilon(r \le R_\mathrm{e}) = \varepsilon_0$, after which it decreases as

$$\varepsilon(r > R_\mathrm{e}) = \varepsilon_0\left(\frac{R_\mathrm{e}}{r}\right)^{p_3} \tag{4}$$

Additionally, we introduce a random velocity component, assuming that it is changing across the emission region, i.e. increasing while the outflowing material is accelerating and decreasing afterwards. Thus, the maximum of the random velocity occurs at the radius R_a. Thus, we have for the random velocity V_ran:

$$V_\mathrm{ran}(r) = \left\{ \begin{array}{l} V_\mathrm{ran}^\mathrm{max}\sqrt{\frac{r}{R_\mathrm{a}}},\ r < R_\mathrm{a} \\ V_\mathrm{ran}^\mathrm{max}\sqrt{\frac{R_\mathrm{a}}{r}},\ r > R_\mathrm{a} \end{array} \right\} \tag{5}$$

where $V_\mathrm{ran}^\mathrm{max}$ is the maximal random velocity.

Moreover, we took into account the inflow of matter which is caused by the gravity, so this velocity can be calculated using the gravitational redshift, which is given as (see e.g. Corbin 1997)

$$\frac{\Delta\lambda_g(r)}{\lambda_0} = -\left(-1 + \sqrt{1 - \frac{2}{r}}\right) \tag{6}$$

where the minus is due to the chosen reference frame described above.

At the end, we calculate the total line profile assuming that contributions from each individual component of the BLR to the broad line profile can be represented by the Gaussian function. The resulting line profile is then given by

$$I(\lambda) = \frac{1}{R_\mathrm{o}-R_\mathrm{i}}\int_{R_\mathrm{i}}^{R_\mathrm{o}} \varepsilon(r)\cdot e^{-F(r)}dr \tag{7}$$

where $F(r)$ is defined as

$$F(r) = \left(\frac{\lambda-\lambda_0-\Delta\lambda_r(r)-\Delta\lambda_g(r)}{W(r)}\right)^2 \tag{8}$$

Here $\Delta\lambda_r(r)$ determines the radial velocity in the following way

$$\Delta\lambda_r(r) = \frac{V(r)}{c}\lambda_0 \tag{9}$$

and $W(r)$ gives the random velocity as

$$W(r) = \frac{V_\mathrm{ran}(r)}{c}\lambda_0 \tag{10}$$

The velocity due to gravitational field is defined through the gravitational redshift as

$$\Delta\lambda_g(r) = \frac{V_\mathrm{g}(r)}{c}\lambda_0 \tag{11}$$

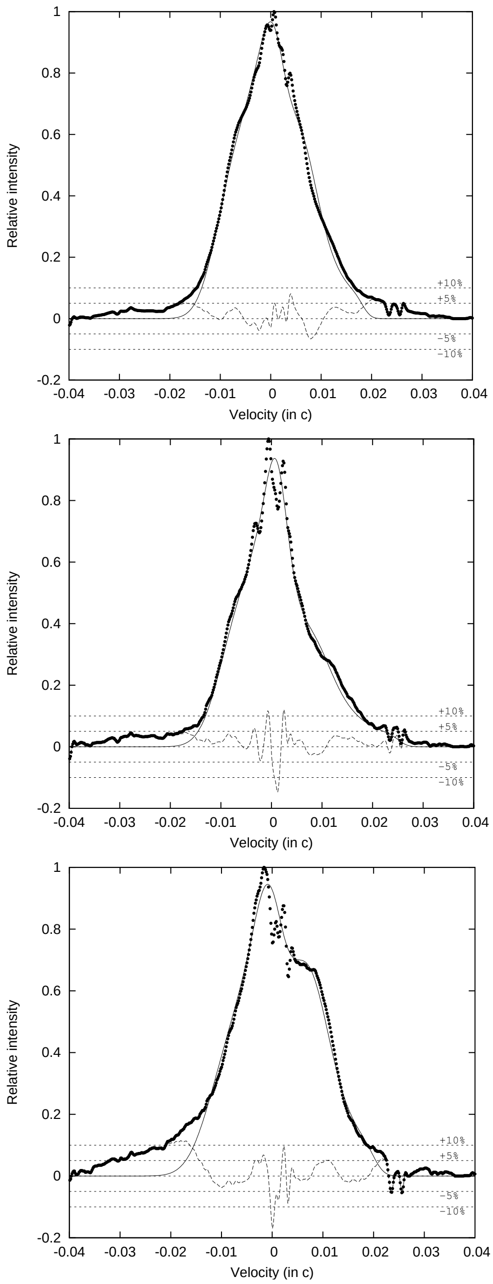

Fig. 2. The outflow model (solid line) in comparison with the averaged Hα line shape (dots) for NGC 4151 for each characteristic period: period I (top panel), II (middle panel), III (bottom panel).

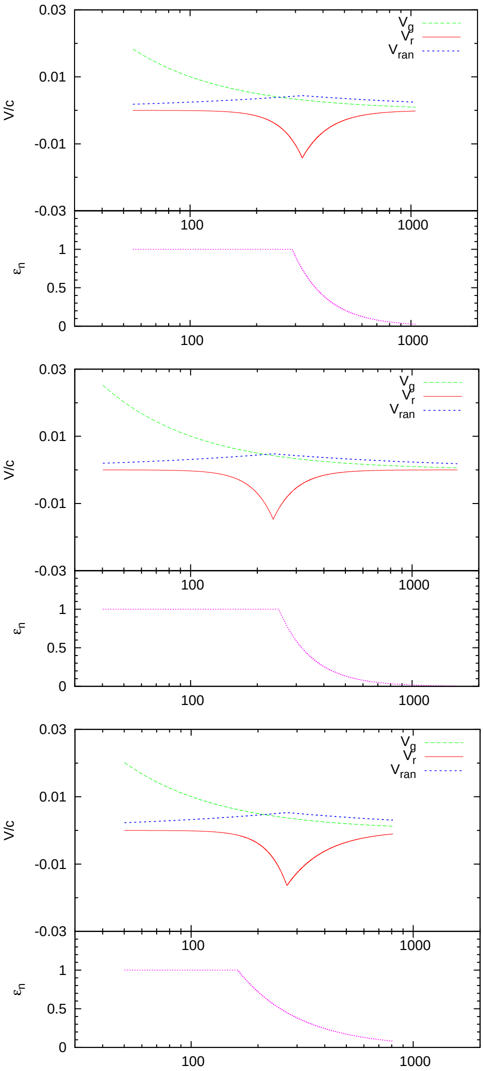

Fig. 3. The assumed velocity fields and the normalized emissivity ε_n for NGC 4151 for each characteristic period: period I (top panel), II (middle panel), III (bottom panel).

3. The case of NGC 4151

Using the model described above, we fitted the average Hα line from three periods introduced by Shapovalova et al. (2008). Since the absorption is much larger in the Hβ line, we will try to fit only the Hα profiles averaged for three characteristic periods (see Shapovalova et al.

2008, 2009b, for details). We assumed that in all three cases the starting velocity of acceleration is very small ($V_0 \sim 1$ km s^{-1}), and that the emission is starting from $\sim 50\,R_{\rm g}$. The best fitting results are given in Table 1 and Figs. 2-3. Fig. 2 gives the corresponding average profile of the Hα line for all three periods, while Fig. 3 represents the velocity fields and the normalized emissivity $\varepsilon_{\rm n}$ of the corresponding periods. As it can be seen from the residuals, also given in Fig. 2, the model is describing well the observed averaged line profiles. The total flux of the observed and modeled line differs at most by 3%, while some line parts can differ by up to 10% (Fig. 2).

Note here that it is hard to fit all substructures in the broad lines with the model (see Fig. 2). This is worst in the individual line profiles. But in general, one can conclude that the model fits correctly the observed line profiles.

4. Conclusions

Taking into account that the BELs of NGC 4151 are highly variable both in flux and profile (Shapovalova et al. 2008, 2009a,b), i.e. that the BLR is having a complicated and variable structure, we apply the outflow model to the averaged broad Hα profiles for three different periods. From the fitting we can conclude that:

1) The accelerating outflow model gives a satisfying agreement between the averaged observed and modeled Hα profiles, but there are some details in individual profiles (bumps) that seems to originate in additional substructures.

2) The extracted outflow parameters are similar for all three periods, but give a bit faster outflow in the period III when it was the minimum of NGC 4151 activity (Shapovalova et al. 2009b); this may indicate that in some periods the obscuration of the continuum source is higher (i.e. when the ejection of material from the center is more effective).

3) The size of the BLR coming from the model-fitting, if we adopt the black hole mass of $4{\times}10^7\ M_\odot$ (see e.g. Onken et al. 2007), is ~ 0.02 l.d., which is in agreement with the previous estimates, that give the BLR size in an interval of 0-2 days (see e.g Shapovalova et al. 2008 and reference therein).

In future work, we are going to test the outflow model in a sample of AGN which BELs show unusual blue asymmetry.

Acknowledgements. This work is supported by the Ministry of Science of Republic of Serbia through the project Astrophysical Spectroscopy of Extragalactic Objects (146002), INTAS (grant N96-0328), RFBR (grants N97-02-17625 N00-02-16272, N03-02-17123 and 06-02-16843), State program 'Astronomy' (Russia), and CONACYT research grants 39560-F & 54480 (Mexico).

References

Arshakian, T. G. et al. 2009, MNRAS, doi: 0.1111/j.1365-2966.2009.15714.x
Corbin, M. R. 1997, ApJ, 485, 517
Ilić, D. et al. 2008, Mem. S.A.It., 79, 1105
Onken, C. A. et al. 2007, ApJ, 670, 105
Peterson, B. M. 2006, in D. Alloin et al., *Physics of Active Galactic Nuclei at all Scales*, Lect. Notes Phys. 693 (Springer, Berlin Heidelberg 2006)
Sergeev, S. G., Pronik, V. I., Sergeeva, E.A. 2001, ApJ, 554, 245
Shapovalova, A.I. et al. 2008, A&A, 486, 99
Shapovalova, A.I. et al. 2009a, NewAR, 53, 191
Shapovalova, A.I. et al. 2009b, A&A, in press, arXiv:0910.2980
Ulrich, M.-H., 2000, Astro.Astrophys.Rev., 10, 135